

# Input shaping and variable structure control for simultaneous precision positioning and vibration reduction of flexible spacecraft with saturation compensation

Qinglei Hu

*Department of Control Science and Engineering, Harbin Institute of Technology, Harbin 150001, China*

Received 6 July 2007; received in revised form 20 November 2007; accepted 30 March 2008

Handling Editor: L.G. Tham

Available online 23 May 2008

---

## Abstract

This paper treats the question of simultaneous robust attitude control and vibration suppression of orbiting spacecraft with flexible appendages. The spacecraft consists of a rigid body and two flexible appendages and the finite dimensional representation of the flexible spacecraft is assumed to be of arbitrary order. Robust nonlinear variable structure control (VSC) strategy integrated with input shaping technique is concerned for the pitch angle control and elastic vibration suppression under actuator saturation limit. More specially, the input shaper is implemented outside of the feedback loop, which is designed for the reference model and achieves the exact elimination of residual vibration; while for the feedback loop, the variable structure controller is designed to make the closed-loop system behave like the reference model with the input shaper in the presence of parametric uncertainty, external disturbances and actuator saturation. To prevent the presence of input saturation from destroying the system performance, a saturation compensator is designed as well for the variable structure attitude control system. For the synthesis of the attitude controller, only the pitch angle and its derivative are used. Simulation results are presented which show that in the closed loop, pitch angle control and elastic mode stabilization are accomplished in spite of uncertainty and external disturbance.

© 2008 Elsevier Ltd. All rights reserved.

---

## 1. Introduction

One of the most important problems in spacecraft design is that of attitude stabilization and control. Although the missions of space vehicles and their attitude requirements vary greatly, high pointing accuracy is an important part of the overall design problem for a spacecraft control system. Meeting the spacecraft attitude control system design requirements in a realistic environment where the knowledge about the system parameters may be incomplete, disturbances are present and orbital operations induces structural vibrations in the flexible appendages is a challenging task for the designers.

Considerable research related to spacecraft attitude control system design has been done in the past several decades [1–4]. Variable structure control (VSC) scheme has long been recognized as an effective means to

---

*E-mail address:* [huqinglei@hit.edu.cn](mailto:huqinglei@hit.edu.cn)

improve transient response and achieve robust performance and several representative works [5–8] on this topic are available in the literatures. However, in most of these studies concerning VSC, it is assumed that the spacecraft is rigid and no flexible mode actions are considered. For the flexible spacecraft model, finite mathematical discretization was used to design sliding mode controllers and there have been significant research efforts for the general feedback attitude control of flexible spacecraft [9–11]. In a practical situation, the measurements of flexible modes are extremely difficult. Thus, there is a need to design a control system for torque control, which does not require the measurement of all state variables. Based on output feedback control concept, controllers for maneuvering the flexible spacecraft have been designed in Refs. [12–14]. However, in this approach, the structure of the uncertainty, which is determined by the number of vibration modes included in the model, is to be known in the controller design. Moreover, in their effort, this disturbance vector has a special structure that may limit its applicability to many systems, and no parametric uncertainty is considered. Recently, for the uncertain nonlinear system, Lewis [15] presents a general sliding mode output feedback control methodology, which addressed uncertainty in the plant, control, and disturbance matrices, provided certain bounds are known.

A typical feature in all of the mentioned attitude control schemes is that the control device is also assumed to be able to produce big enough control torque to reject the external disturbances and no actuator saturation limits is considered in the controller design. Unfortunately, this requirement is not always satisfied in reality due to the physical structure and energy consumption, and thus there does exist a control saturation limit, which can lead to serious discrepancies between commanded input signals and actual control effort, and is also a source of degradation or, even worse, instability in the performance of the system. Extensive results pertaining to spacecraft attitude control systems containing actuator saturation nonlinearities have been presented by Bošković et al. [16], Tsiotras and Luo [17], Robinett et al. [18], Walls Grove and Akella [19], Bang et al. [20] and references therein.

To reduce vibrations the use of active vibration control technique are investigated as a potential solution to efficiently maneuver lightweight flexible spacecraft and minimize the excitation of structural resonances during operations. One simple and special feed-forward control strategy, known as input shaping, has been studied widely since its first appearance [21] for possessing the advantages of simplicity and effectiveness, and because no additional sensor and actuator are required. With this method, an input command is convolved with a sequence of impulses, called an input shaper, to produce a shaped command that causes less vibration than the original unshaped command. Singhose et al. [22] studied an input shaping controller for slewing a flexible spacecraft. Banerjee and Padereiro [23] proposed the application of input shaping for vibration reduction of flexible spacecraft following momentum damping with/without slewing. Hillsley and Yurkovich [24,25] apply input shaping to large angle movements of a two-link robot, switched to feedback control when approaching the desired position. Chang and Park [26] treated the application of time-varying input shaping for vibration reduction of an industrial robot. Modified input shaping was presented in Ref. [27] for multimode vibration suppression of a rotating single-link flexible manipulator. In Ref. [28], a new approach integrating component synthesis vibration suppression based command shaping technique and positive position feedback control is proposed for flexible spacecraft attitude maneuver. Nonlinear input shaping technique was considered by Gorinevsky and Vukovich [29] for the flexible spacecraft reorientation maneuver as well. An adaptive input shaper providing robustness to parameter uncertainties by tuning the shaper to the flexible mode frequencies is explored in Ref. [30].

The contribution of this work lies in the derivation of a nonlinear control law for the attitude maneuver control and input shaping for vibration reduction of an orbiting flexible spacecraft in the presence of external disturbances, parameter uncertainties and control input saturation. Although the design method is applicable to spacecraft of other configurations, here an orbiting spacecraft consisting of a rigid hub with two flexible appendages is considered for system design. Based on input shaping technique, the input shaper is designed outside of the feedback loop such that the exact elimination of residual vibration can be achieved. The amplitudes and instances of the impulses application can be obtained for the natural frequency and damping ratio of the reference model, respectively. In the feedback loop, the VSC strategy using only output information is employed to make the closed-loop system behave like the reference system with input shaper and suppress the vibration of the flexible structures in the presence of parametric uncertainty and external disturbances. Moreover, a compensator design is also presented for preventing the presence of input

saturation from deteriorating the system performance. Lyapunov stability analysis shows that the proposed control guarantees asymptotical convergence of attitude angle and angular velocity in the presence of bounded parameter variation/disturbances and even actuator saturation limits. Simulation results are also provided to compare the proposed controller with a conventional proportional-integral-derivative (PID) with anti-windup controller. The paper is organized as follows. The next section states flexible spacecraft modeling. The principle of input shaping and the attitude control system design is described in Section 3. Section 4 presents and analyzes the simulation results. Section 5 concludes the paper.

**2. Mathematical model of a flexible spacecraft**

The flexible spacecraft model under consideration is shown in Fig. 1. The model consists of a rigid central hub, which represents the spacecraft body, and two flexible appendages, which represent antennas, solar arrays, or any other flexible structures. This model is representative of a relatively large class of spacecraft employed for communication, remote sensing or numerous other applications [3,13,14]. Define the OXYZ and oxyz as the inertial frame and the frame fixed on the hub, respectively. Denote  $w(x, t)$  as the flexible deformation at point  $x$  with respect to the oxy frame, and  $l$  is the distance of a point chosen on the appendage from the center of the hub.

The equations of motion are derived using the Lagrangian approach. Although the vibration of the appendages is described by partial differential equations, spatial discretization method is used to obtain a set of ordinary differential equations to describe the motion of the spacecraft. For spatial discretization using assumed modes method, the transverse elastic deflection of the appendage along  $y$  in the oxyz plane is expressed as

$$w(x, t) = \sum_{i=1}^N \phi_i(x)q_i(t) \tag{1}$$

where  $\phi_i(x)$  ( $i = 1, 2, \dots, N$ ) are the chosen admissible functions which satisfy the geometric and physical boundary conditions, and  $q_i(t)$  are the generalized coordinates for the flexible deflection. It is assumed here that  $N$  modes are sufficient for the computation of elastic deformation.

These nonlinear differential equations describing the rotational and elastic dynamics are given by [3]

$$J\ddot{\theta} + M_{\theta q}\ddot{q} = T_h + d \tag{2a}$$

$$M_{\theta q}^T\ddot{\theta} + M_{qq}\ddot{q} + C_{qq}\dot{q} + K_{qq}q = 0 \tag{2b}$$

where  $q = [q_1, q_2, \dots, q_N]^T$ , the element mass, stiffness matrices and the nonlinear terms are governed by  $J = J_h + 2 \int_b^l \rho x^2 dx + 2m_i l^2$ ,  $[K_{qq}]_{ij} = 2 \int_b^l E I \phi_i''(x)\phi_j''(x) dx$ ,  $[M_{qq}]_{ij} = 2 \int_b^l \rho \phi_i(x)\phi_j(x) dx + 2m_i \phi_i(l)\phi_j(l)$ , and  $[C_{qq}]_{ij} = 2 \int_b^l \underline{C} I \phi_i''(x)\phi_j''(x) dx$ . Here,  $\underline{C}$  and  $E$  are the damping coefficient and modulus of elasticity, respectively, for the appendages and  $I$  is the sectional area moment of inertia with respect to the appendage

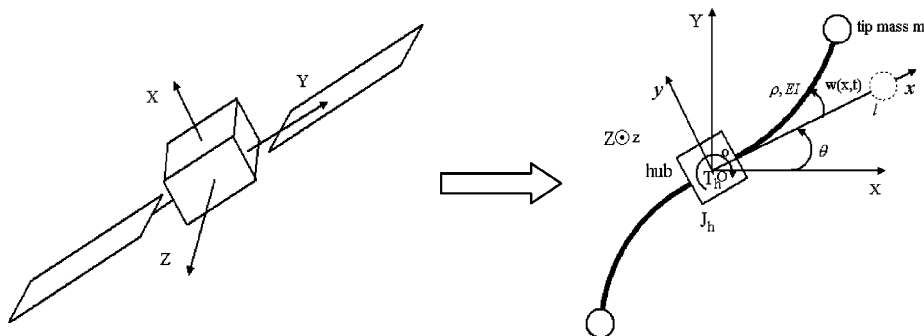


Fig. 1. Spacecraft model with single-axis rotation.

bending axis, and  $d(t) \in R$  is the external disturbances which belong to  $L_2[0, \infty)$  and  $\|d(t)\| \leq \delta_d$  where  $\delta_d$  is a known positive constant.

Eq. (2) can be written in a compact form as

$$\overline{M} \ddot{\overline{Z}} + \overline{C} \dot{\overline{Z}} + \overline{K} \overline{Z} = \overline{B}(T_h + d(t)) \tag{3}$$

where

$$\overline{Z} = [\theta, q^T]^T \in R^{N+1}, \quad \overline{M} = \begin{bmatrix} J & M_{\theta q} \\ M_{\theta q}^T & M_{qq} \end{bmatrix}, \quad \overline{C} = \text{diag}\{0, C_{qq}\}, \quad \overline{K} = \text{diag}\{0, K_{qq}\}, \quad \overline{B} = \begin{bmatrix} 1 \\ 0 \end{bmatrix}$$

and 0 denotes a null vector of appropriate dimension.

The system of  $\overline{Z}$  second-order differential equations, Eq. (3) can be transformed into the state-space form

$$\dot{x} = Ax + B\overline{u}(t) + Bd(t) \tag{4}$$

where

$$x = \begin{bmatrix} \overline{Z} \\ \dot{\overline{Z}} \end{bmatrix}, \quad A = \begin{bmatrix} 0 & I \\ -\overline{M}^{-1}\overline{K} & -\overline{M}^{-1}\overline{C} \end{bmatrix}, \quad B = \begin{bmatrix} 0 \\ \overline{M}^{-1}\overline{B} \end{bmatrix}, \quad \overline{u}(t) = T_h.$$

In this work, we are interested in deriving a control system such that in the closed-loop system, the pitch angle  $\theta(t)$  is rotated from initial state to  $\theta_d \in [0, 2\pi]$ , for example, setting to  $60^\circ$ , in the presence of external disturbance and parametric uncertainty, and at the same time, the induced elastic oscillations are actively damped out. For the design of the controller, it is assumed that the synthesis of the controller must also be done using only the measured signals  $\theta$  and  $\dot{\theta}$ , since the elastic modes  $q$  and  $\dot{q}$  are not available. In addition, it is desired that the structure of the attitude control law must be independent of the dimension of the spacecraft model. This is important since the flexible structures have infinite dimension, but of then finite dimensional truncated models are considered for analysis and design.

### 3. Control system design

This paper focuses on simultaneous precision positioning and vibration suppression of flexible spacecraft during attitude maneuvering. The introduced control strategy consists of input shaping unit and robust VSC unit with saturation compensator, and both units are designed separately, as shown in Fig. 2. The input shaping unit is implemented outside of the feedback loop and used to suppress induced vibration of the reference model due to orbital operations. The attitude control unit based on variable structure output

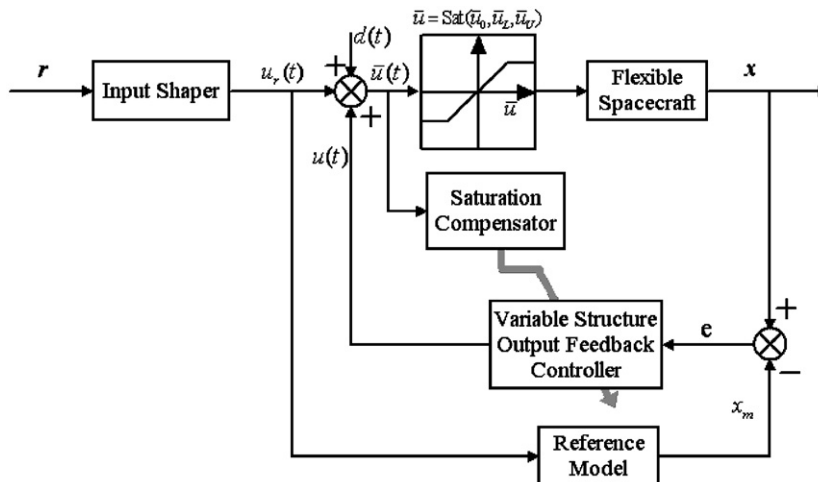


Fig. 2. A block-diagram of variable structure/input shaping algorithm for flexible spacecraft vibration reduction.

feedback control (VSOFC) theory then provides precision positioning control and robust to external disturbances and uncertain. This is an effective method of implementing input shaping for satisfactory performance and robustness even when parameter variations and external disturbance occur simultaneously in the process. In addition, an internal saturation compensator is employed to compensate the actuator saturation, which imposes limitations on the magnitude of the control input, such that the system performance can be guaranteed. The following systematic design procedure will be provided for designing the system.

### 3.1. Input shaping technique

In the method of input shaping [21], an input command is convolved with a sequence of impulses, an input shaper, designed to produce a resulting input command that causes less residual vibration than the original unshaped command. This is, any vibration induced by the first part of the command is canceled by vibration induced by a later portion of the command, and the result of the convolution is then used to derive the system. The convolution can be pre-computed if the entire unshaped input is known, or more likely, it can be computed in real time from the input command generator. The impulses that constitute the shaper must have appropriate amplitudes and time locations, which are determined by solving a set of constraint equations, which can generally be categorized as residual vibrations constraints, robustness constraints, constraints on the impulse amplitudes, or time optimality requirements. This method is briefly described in this section, see e.g., Refs. [21–30] for details.

For a linear second-order system

$$G(s) = \frac{\omega^2}{s^2 + 2\zeta\omega + \omega^2} \quad (5)$$

with natural frequency  $\omega$  and damping ratio  $\zeta$ . Then, for system (5), the response to a sequence of  $\bar{N}$  impulses is described as

$$Y(t) = \sum_{i=1}^{\bar{N}} \left[ \frac{A_i \omega}{\sqrt{1 - \zeta^2}} e^{\zeta\omega(t-t_i)} \sin\left(\omega\sqrt{1 - \zeta^2}(t - t_i)\right) \right] \quad (6)$$

where  $A_i$  and  $t_i$  are the amplitude and the application time of the  $i$ th impulses, respectively; these are the parameters to be determined for the input shaping technique design by using the following constraints, Eqs. (7a) and (7b), derived from Eq. (6)

$$\sum_{i=1}^{\bar{N}} \left[ A_i t_i^p e^{-\zeta\omega(t_{\bar{N}}-t_i)} \sin\left(t_i \omega \sqrt{1 - \zeta^2}\right) \right] = 0 \quad (7a)$$

$$\sum_{i=1}^{\bar{N}} \left[ A_i t_i^p e^{-\zeta\omega(t_{\bar{N}}-t_i)} \cos\left(t_i \omega \sqrt{1 - \zeta^2}\right) \right] = 0 \quad (7b)$$

where  $p = 0, 1, \dots, \bar{N} - 2$ . The above two constraints were derived from the requirements that the amplitude of  $Y(t)$  and its derivatives (with respect to  $\omega$ ) be made zero for  $t > t_{\bar{N}}$ , which imply zero amplitude of vibration after  $t_{\bar{N}}$ . From Ref. [21],  $A_i$  and  $t_i$  can be concluded as follows:

$$A_i = \frac{\binom{\bar{N}-1}{i-1} K^{i-1}}{\sum_{j=0}^{\bar{N}-1} \binom{\bar{N}-1}{j} K^j}, \quad t_i = (i-1) \frac{\pi}{\omega \sqrt{1 - \zeta^2}}, \quad i = 1, \dots, \bar{N} \quad (8)$$

where  $K = \exp\left[-(\pi\zeta)/(\sqrt{1 - \zeta^2})\right]$ . Note that the input shaper impulse sequences can also be generalized to consider more than one vibration mode, by convolving the impulse sequences for each individual mode with

one another. Let the input with  $\bar{N}_j (j = 1, \dots, n) (n > 1)$  impulses be used in the  $j$ th mode. After the necessary convolutions, the input impulse sequences,  $A_{\text{mult}}$ , can be expressed:

$$A_{\text{mult}} = A_{1s} * A_{2s} \cdots * A_{ns} \quad (9)$$

where  $A_{js}$  is the impulse sequences of the  $j$ th mode of the system with  $\bar{N}_j$  impulses, and  $*$  is the convolution operator.

**Remark 1.** In this manner, for a vibratory system, the described impulse sequence can be convolved to an arbitrary input, to obtain the same vibration-reducing properties of the impulsive input case. In addition, the same expressions that guarantee vibration-reducing properties of the constraints with respect to frequency also guarantee vibration-reducing properties with respect to damping ratio. Moreover, the high variations in damping ratio can be tolerated.

From above analysis, it is known that the input shaper is an open-loop controller, which has the limitation in coping with parameter changes and disturbances to the system. Moreover, this technique requires relatively precise knowledge of the dynamics of the system. Even if several design approaches have been proposed to improve the robustness of input shaping to the damping factors and natural frequencies of the flexible structure [27–29]. It should also be noted that the plant being linear is essential for proving why the input shaping technique works. In this work, the input shaping is applied in conjunction with the VSC for maneuvers of flexible spacecraft. The preliminary results that indicate such control architecture, which provides very good performance, will be shown in the next sub-section.

### 3.2. Variable structure attitude controller design

From Fig. 2, system (4) can be rewritten as

$$\dot{x} = Ax + Bu(t) + Bu_r + Bd(t) \quad (10)$$

where  $\bar{u}(t) = u(t) + u_r(t)$ . Here, the reference model is selected as the nominal system. The combination of the input shaper convolving with the reference model dynamics can be expressed as

$$\dot{x}_m = A_m x_m + B_m u_r \quad (11)$$

where  $A_m$  and  $B_m$  are the known matrices of the nominal system. According to the principle of the input shaping technique, the shaped input  $u_r$  can be expressed as

$$u_r = r(t) * A_{\text{mult}} \quad (12)$$

where  $*$  is the convolution operator. Then applying convolution operator, one can rewrite Eq. (12) as

$$u_r = \left( \prod_{j=1}^n A_{j,1} \right) r(t) + X_{1,2} \left( \prod_{j=2}^n A_{j,1} \right) r(t - t_{1,2}) + \cdots + \left( \prod_{j=1}^n A_{j,\bar{N}_j} \right) r \left( t - \sum_{j=1}^n t_{j,\bar{N}_j} \right) \quad (13)$$

To simplify notation, Eq. (13) can be written as

$$u_r = \sum_{k=0}^{2n-1} a_k r(t - t_k) \quad (14)$$

where

$$a_0 = \prod_{j=1}^n A_{j,1}, \quad a_1 = A_{1,2} \prod_{j=2}^n A_{j,1}, \dots, a_{2n-1} = \prod_{j=1}^n A_{j,\bar{N}_j}, \quad t_0 = 0, t_1 = t_{1,2}, \dots, t_{2n-1} = \sum_{j=1}^n t_{j,\bar{N}_j}.$$

Substituting Eq. (14) into Eqs. (11) and (12), the following equations can be obtained:

$$\dot{x} = Ax + Bu(t) + B \left[ \sum_{k=0}^{2n-1} a_k r(t - t_k) \right] + Bd(t) \quad (15)$$

$$\dot{x}_m = A_m x_m + B_m \left[ \sum_{k=0}^{2n-1} a_k r(t - t_k) \right] \quad (16)$$

The parameter variations of the system considered here are defined as follows. The parameter uncertainties of the system,  $\Delta A$ , can be expressed as

$$\Delta A = A - A_m \quad (17)$$

It is noted that in this work the uncertainty matrix  $\Delta A$  need not satisfy the so-called matching condition. However, the uncertainty in the input is assumed to satisfy the matching condition and can be expressed as

$$\Delta B = B - B_m = B_m D_B \quad (18)$$

Introducing  $e(t) = x(t) - x_m(t)$  into Eqs. (15) and (16), the error dynamics are expressed in terms of the error state vector  $e(t)$ :

$$\dot{e} = (A_m + \Delta A)e + B_m(I + D_B)u + \Delta A x_m + B_m D_f \quad (19)$$

where  $D_f = D_B \sum_{k=0}^{2n-1} a_k r(t - t_k) + (I + D_B)d$ .

It is assumed in this study that the attitude angle and angular velocity are measurable, and the elastic modes are unavailable. The measurement available for the controller design can be expressed in the output form as

$$y = Ce \quad (20)$$

where  $y \in R^p$  and  $C$  is an appropriately dimensioned matrix.

Throughout the remainder of this paper, the following assumptions are taken to be valid:

**Assumption 1.** The triplet  $(A_m, B_m, C)$  is controllable and observable.

**Assumption 2.** There exist known constants  $\delta_A$  and  $\delta_B$  such that the uncertainties,  $\Delta A$  and  $\Delta B$  in Eqs. (17) and (18), are known but bounded as  $\|\Delta A\| \leq \delta_A$  and  $\|D_B\| \leq \delta_B$ .

**Remark 2.** If it is possible to design a control law that makes the error dynamics (19) have a stable zero steady-state solution, i.e.,  $e(t) \rightarrow 0 \rightarrow x(t) \rightarrow x_m(t)$ , then the closed-loop system will exactly eliminated the residual vibration like the reference model. Since sliding mode control provides good ability to reject disturbances and remain robust to parameter perturbations while tracking a desired trajectory, it can be more useful for this purpose than other strategies in the literature.

In order to simplify the development of the control design scheme, the following state transformation is applied:

$$\bar{e}(t) = Te(t) \quad (21)$$

with  $T^{-1} = T^T$ . The transformed equations with  $\bar{e}^T = [\bar{e}_1^T \quad \bar{e}_2^T]^T$ ,  $\bar{e}_1 \in R^{n-m}$  and  $\bar{e}_2 \in R^m$ , are

$$\dot{\bar{e}}_1 = (A_{11} + \Delta A_{11})\bar{e}_1 + (A_{12} + \Delta A_{12})\bar{e}_2 + [\Delta A_{11m} \quad \Delta A_{12m}]x_m(t) \quad (22a)$$

$$\dot{\bar{e}}_2 = (A_{21} + \Delta A_{21})\bar{e}_1 + (A_{22} + \Delta A_{22})\bar{e}_2 + [\Delta A_{21m} \quad \Delta A_{22m}]x_m(t) + B_2(I + D_B)u + B_2 D_f \quad (22b)$$

$$Y = CT^T \bar{e} = C_1 \bar{e}_1 + C_2 \bar{e}_2 \quad (22c)$$

where

$$\begin{bmatrix} A_{11} & A_{12} \\ A_{21} & A_{22} \end{bmatrix} = TA_m T^T, \quad \begin{bmatrix} \Delta A_{11} & \Delta A_{12} \\ \Delta A_{21} & \Delta A_{22} \end{bmatrix} = T \Delta A T^T, \quad \begin{bmatrix} \Delta A_{11m} & \Delta A_{12m} \\ \Delta A_{21m} & \Delta A_{22m} \end{bmatrix} = T \Delta A \quad \text{and} \quad TB_m = \begin{bmatrix} 0 \\ B_2 \end{bmatrix}.$$

### 3.2.1. Switching surface design

In the following, the design of a variable structure attitude control system is considered. Essential to the design of a variable structure controller is the selection of switching surface; then the control law is designed such that all the trajectories are attracted towards this surface and after reaching the surface they slide on it.

The structure of the controller changes when the trajectory crosses the switching surface. For the purpose of design, select a switching surface  $S(t)$  in the error state space [15,31,32]

$$S = (GC_2)^{-1}Gy = (GC_2)^{-1}GC_1\bar{e}_1 + \bar{e}_2 \tag{23}$$

where the matrix  $G \in R^{m \times p}$  is selected by the designer,  $S \in R^m$  and  $(GC_2)$  is assumed to be invertible. Eq. (23) can be rewritten to express  $\bar{e}_2$  in terms of  $\bar{e}_1$  and  $S$  as

$$\bar{e}_2 = S - (GC_2)^{-1}GC_1\bar{e}_1 \tag{24}$$

Substituting Eqs. (24) into Eq. (22) gives

$$\dot{\bar{e}}_1 = A_r\bar{e}_1 + (A_{12} + \Delta A_{12})S + [\Delta A_{11m} \quad \Delta A_{12m}]x_m(t) \tag{25a}$$

$$A_r = A_{11} - A_{12}(GC_2)^{-1}GC_1 + \Delta A_{11} - \Delta A_{12}(GC_2)^{-1}GC_1 \tag{25b}$$

Note that  $G$  must be chosen to ensure that the eigenvalue of the reduced-order matrix  $A_r$ , i.e.,  $\{-\lambda_1, -\lambda_2, \dots, -\lambda_{n-m}\}$  (real part of  $\lambda_i > 0$ ) are stable. Even if  $A_r$  has uncertainties associated with it, they are assumed to be bounded. Conditions were given in Refs. [15,31,32], in the absence of uncertainty for how to choose  $G$  so that  $(n-m)$  prescribed non-zero and complex eigenvalues  $\{-\lambda_1, -\lambda_2, \dots, -\lambda_{n-m}\}$  with  $\text{Re}(\lambda_i) > 0 (i = 1, 2, \dots, n - m)$  can be assigned, namely, arbitrary pole placement is possible if

$$\text{rank}[C_2(GC_2)^{-1}G - I] \leq p - m \tag{26}$$

However, if this condition is not satisfied, it still may be possible to achieve stable poles even in the presence of uncertainty, but they may not be arbitrary. With a stable  $A_r$  matrix having been determined, the eigenvalues of  $A_r$  can be grouped as  $\{-\lambda_1, -\lambda_2, \dots, -\lambda_{n-m}\}$ . The following lemma shows that

$$\|\exp(A_r t)\| \leq \gamma \exp(-\lambda_{\min} t) \tag{27}$$

where  $\lambda_{\min} > 0$  is the minimum real part of the  $\lambda_i$  and  $\gamma > 0$ . Thus, the important issue with this design is being able to determine  $\lambda_{\min}$  given a stable set of eigenvalues.

**Lemma 1.** Consider Eq. (25a). Let  $\lambda_{\min} > 0$  be the minimum real part of  $\{-\lambda_1, \lambda_2, \dots, \lambda_{n-m}\}$ . Then we have the following.

- (1) The  $\|\exp(A_r t)\| \leq \gamma \exp(-\lambda_{\min} t)$  for some  $\gamma > 0$ .
- (2) Also,  $\|\bar{e}_1\|$  is bounded by  $w(t)$  after a finite period of time with  $w(t)$  the solution of

$$\dot{w}(t) = -\lambda_w w(t) + \gamma \left[ \|(A_{12} + \Delta A_{12})\| \|S\| + d^* \right] \tag{28}$$

where  $w(0) > 0$ ,  $\lambda_w < \lambda_{\min}$  and  $\|[\Delta A_{11m} \quad \Delta A_{12m}]x_m(t)\| < d^*$ .

**Proof.** The proof is straightforward and follows directly from the same arguments as in Refs. [31,32]. □

### 3.2.2. Variable structure output feedback controller design

By the use of Eq. (23), the time derivatives of  $S$  is given by

$$\dot{S} = (GC_2)^{-1}G\dot{y} = (GC_2)^{-1}GC_1\dot{\bar{e}}_1 + \dot{\bar{e}}_2[P\bar{e}_1 + QS + R + B_2(I + D_B)u] \tag{29}$$

where the matrices  $Q$ ,  $R$  and  $P$  are defined as, respectively,  $Q = (GC_2)^{-1}GC_1(A_{12} + \Delta A_{12}) + (A_{22} + \Delta A_{22})$ ,  $R = (GC_2)^{-1}GC_1[\Delta A_{11m} \quad \Delta A_{12m}]x_m(t) + [\Delta A_{21m} \quad \Delta A_{22m}]x_m(t) + B_2 D_f$  and  $P = (GC_2)^{-1}GC_1[A_{11} + \Delta A_{11} - (A_{12} + \Delta A_{12})(GC_2)^{-1}GC_1] + A_{21} + \Delta A_{21} - (A_{22} + \Delta A_{22})(GC_2)^{-1}GC_1$ .

In this work, the desired control law is chosen in the form

$$u = B_2^{-1}(I - \overline{\overline{D}}_B)^{-1}[-Hw(t) - \Pi\|S\| - \delta - \eta]\text{sgn}(S) \tag{30}$$

where  $H \geq \|P\|$ ,  $\Pi \geq \|Q\|$ ,  $\delta_i \geq \sup(R)_i$ ,  $\eta_i > 0$ ,  $i = 1, 2, \dots, m$ ,  $\overline{\overline{D}}_B$  is defined as  $\overline{\overline{D}}_B = (B_2 D_B)B_2^{-1}$  and the term “ $\text{sgn}(\bullet)$ ” is the sign function. Then the stability analysis result is given in the following.



**Theorem 1.** Consider the uncertain system (22) subjected to Assumption 1 and 2. If the input control  $u(t)$  in Eq. (22) is given as that indicated by Eq. (30), then  $\dot{V} \leq -\sum_{i=1}^m \eta_i |s_i| < 0$  holds and the closed-loop satisfies  $S$ ,  $\dot{S}$  and  $e$  are bounded and  $e \rightarrow 0$  as  $t \rightarrow \infty$ .

**Proof.** Consider the Lyapunov function candidate:

$$V = \frac{1}{2} S^T S \quad (31)$$

Differentiating the Lyapunov function  $V$  gives

$$\dot{V} = S^T \dot{S} = S^T [P\bar{e}_1 + QS + R + B_2(I + D_B)u] \quad \square \quad (32)$$

Using the swapping technique similar to that of Kan [32] by rearranging  $B_2(I + D_B)$  to the form of  $(I + \bar{D}_B)B_2$ , one can obtain the following:

$$\dot{V} = S^T \dot{S} = S^T [P\bar{e}_1 + QS + R + (I + \bar{D}_B)B_2u] \quad (33)$$

Defining vectors  $f \triangleq P\bar{e}_1 + QS + R$  and  $\bar{K} \triangleq (\bar{I} - \bar{D}_B)^{-1} [Hw(t) + \Pi \|S\| + \delta]$ , then controller (30) simplifies to

$$u = -B_2^{-1} \bar{K}(t) \text{sgn}(S) \quad (34)$$

and substituting control  $u$  in Eq. (34) into Eq. (33) yields

$$\begin{aligned} \dot{V} &= S^T [f - (I + \bar{D}_B) \bar{K}(t) \text{sgn}(S)] \\ &= \sum_{i=1}^m s_i \left[ f_i - \sum_{j \neq i} (\bar{D}_B)_{ij} \bar{K}_j(t) \text{sgn}(s_j) - [1 + (\bar{D}_B)_{ii}] \bar{K}_i(t) \text{sgn}(s_i) \right] \end{aligned} \quad (35)$$

It can be seen that sliding condition holds if

$$[1 - (\bar{D}_B)_{ii}] \bar{K}_i(t) \geq L_i + \eta_i + \sum_{j \neq i} (\bar{D}_B)_{ij} \bar{K}_j(t), \quad i = 1, 2, \dots, m \quad (36)$$

with  $\bar{D}_B$  defined in Eq. (30) and  $\|f_i\| \leq Hw(t) + \Pi \|S\| + \delta_i \triangleq L_i$ . Note that sliding condition also holds if vector  $\bar{K}(t)$  is chosen such that

$$[1 - (\bar{D}_B)_{ii}] \bar{K}_i(t) = L_i + \eta_i + \sum_{j \neq i} (\bar{D}_B)_{ij} \bar{K}_j(t), \quad i = 1, 2, \dots, m \quad (37)$$

Eq. (37) contains a set of  $m$  equalities with  $m$  switching gains  $\bar{K}_i$ . Using matrix notation, Eq. (37) is equivalent to

$$[I - \bar{D}_B] \bar{K}(t) = L + \eta \quad (38)$$

Using Frobenius–Perron theorem [33], then a unique and positive solution for  $\bar{K}(t)$  exists and is given by

$$\bar{K}(t) = [I - \bar{D}_B]^{-1} (L + \eta) \quad (39)$$

Submitting Eq. (39) into Eq. (35) and noting  $w(t) \geq \|\bar{e}_1(t)\|$  from Lemma 1, it can be verified that

$$\begin{aligned} \dot{V} &= \sum_{i=1}^m s_i \left\{ f_i - \sum_{j \neq i} (\bar{D}_B)_{ij} \bar{K}_j(t) \text{sgn}(s_j) - \frac{[1 + (\bar{D}_B)_{ii}]}{[1 - (\bar{D}_B)_{ii}]} \left[ L_i + \eta_i + \sum_{j \neq i} (\bar{D}_B)_{ij} \bar{K}_j(t) \right] \text{sgn}(s_i) \right\} \\ &= \sum_{i=1}^m s_i \left\{ f_i - \frac{[1 + (\bar{D}_B)_{ii}]}{[1 - (\bar{D}_B)_{ii}]} [L_i + \eta_i] \text{sgn}(s_i) - \left\{ \sum_{j \neq i} (\bar{D}_B)_{ij} \bar{K}_j(t) \text{sgn}(s_j) \right. \right. \\ &\quad \left. \left. + \frac{[1 + (\bar{D}_B)_{ii}]}{[1 - (\bar{D}_B)_{ii}]} (\bar{D}_B)_{ij} \bar{K}_j(t) \text{sgn}(s_i) \right\} \right\} \\ &\leq -\sum_{i=1}^m \eta_i |s_i| \end{aligned} \quad (40)$$

Since  $V$  is positive definite and  $\dot{V}$  is negative semi-definite, therefore,  $S, e \in L_\infty$  and  $S$  asymptotically converges to zero. Also, the fact  $\dot{S}, \ddot{S} \in L_\infty$  due to the bounded perturbations and that  $S$  is convergent imply that  $\dot{S}$  asymptotically converges to zero by Barbalat's lemma. Thus, the closed-loop system approaches the union of  $S(t) = 0$  and  $\dot{S}(t) = 0$  in an asymptotic fashion. In other words  $\lim_{t \rightarrow \infty} e = 0$ .

### 3.3. Variable structure output feedback controller design with saturation compensator

From a practical perspective, one of the major issues in above attitude control system design is that the signal  $\bar{u}(t)$  generated by the control law might not be implemented because of physical constraints. A common example of such a constraint is actuator saturation, which imposed limitations on the magnitude of the achievable control input. When the actuator saturation is considered, the actual attitude control being implemented is different from Eq. (30) with Eq. (28) as follows:

$$\bar{u} = \text{sat}(\bar{u}_0, \bar{u}_L, \bar{u}_U) \tag{41a}$$

$$\bar{u}_0 = B_2^{-1}(I - \bar{D}_B)^{-1}[-Hw(t) - \Pi\|S\| - \delta - \eta]\text{sgn}(S - \chi) - B_2^{-1}(I + \bar{D}_B)^{-1}\alpha\chi + u_r \tag{41b}$$

$$\dot{\chi} = -\alpha\chi + (I + \bar{D}_B)B_2(\bar{u} - \bar{u}_0) \tag{41c}$$

where  $\chi$  is an auxiliary variable, which is a filtered version of the effect of input saturation on the variable being controller,  $\alpha > 0$  to be selected by the designer and the saturation function ‘‘sat’’ is linear with unity slope between its lower and upper limits, i.e.,

$$\text{sat}(\bar{u}_0, \bar{u}_L, \bar{u}_U) = \begin{cases} \bar{u}_U & \text{if } \bar{u}_0 > \bar{u}_U \\ \bar{u}_0 & \text{if } \bar{u}_L \leq \bar{u}_0 \leq \bar{u}_U \\ \bar{u}_L & \text{if } \bar{u}_0 < \bar{u}_L \end{cases} \tag{42}$$

where  $\bar{u}_L$  and  $\bar{u}_U$  are the constant lower and upper limit bounds, respectively. Note that in the case of no input saturation, then  $\chi$  remains zero and the control law becomes the same as the standard control law described in Eq. (30). In the presence of input saturation,  $\chi$  is non-zero, thus giving rise to an error  $(S - \chi)$ . The stability analysis result is given in the following.

**Theorem 2.** Consider the system (22) with the Assumptions 1–3. If the control law is designed in Eqs. (41a) and (41b), subject to saturation and the auxiliary control is selected as in Eq. (28), then the closed-loop system is asymptotically stable and the attitude  $e \rightarrow 0$ ,  $(S - \chi) \rightarrow 0$  as  $t \rightarrow \infty$ .

**Proof.** Consider the Lyapunov function  $\bar{V} = (S - \chi)^T(S - \chi)$ . Then the time derivative of  $\bar{V}$  is by using the control law in Eqs. (41a) and (41b)

$$\begin{aligned} \dot{\bar{V}} &= (S - \chi)^T[f + (I + \bar{D}_B)B_2(\bar{u} - u_r) - \dot{\chi}] \\ &= (S - \chi)^T[f + (I + \bar{D}_B)B_2(u - u_r) + \alpha\chi - (I + \bar{D}_B)B_2(\bar{u} - u_0)] \\ &= (S - \chi)^T[f + (I + \bar{D}_B)B_2\bar{u}_0 - (I + \bar{D}_B)B_2u_r + \alpha\chi] \end{aligned} \tag{43}$$

Substituting Eq. (41b) into Eq. (43) and using the same manipulations as Eqs. (35)–(40) the time derivative of  $\bar{V}$  becomes

$$\begin{aligned} \dot{\bar{V}} &= \sum_{i=1}^m (s_i - \chi_i) \left[ f_i - \sum_{j \neq i} (\bar{D}_B)_{ij} \bar{K}_j(t) \text{sgn}(s_j - \chi_j) - [1 + (\bar{D}_B)_{ii}] \bar{K}_i(t) \text{sgn}(s_i - \chi_i) \right] \\ &= \sum_{i=1}^m (s_i - \chi_i) \left\{ f_i - \sum_{j \neq i} (\bar{D}_B)_{ij} \bar{K}_j(t) \text{sgn}(s_i - \chi_i) - \frac{[1 + (\bar{D}_B)_{ii}]}{[1 - (\bar{D}_B)_{ii}]} \right. \\ &\quad \left. \times \left[ L_i + \eta_i + \sum_{j \neq i} (\bar{D}_B)_{ij} \bar{K}_j(t) \right] \text{sgn}(s_i - \chi_i) \right\} \end{aligned}$$

$$\begin{aligned}
 &= \sum_{i=1}^m (s_i - \chi_i) \left\{ f_i - \frac{[1 + (\overline{D}_B)_{ii}]}{[1 - (\overline{D}_B)_{ii}]} [L_i + \eta_i] \operatorname{sgn}(s_i - \chi_i) - \left\{ \sum_{j \neq i} (\overline{D}_B)_{ij} \overline{K}_j(t) \operatorname{sgn}(s_j) \right. \right. \\
 &\quad \left. \left. + \frac{[1 + (D_B)_{ii}]}{[1 - (\overline{D}_B)_{ii}]} (\overline{D}_B)_{ij} \overline{K}_j(t) \operatorname{sgn}(s_i - \chi_i) \right\} \right\} \\
 &\leq - \sum_{i=1}^m \eta_i |s_i - \chi_i|
 \end{aligned} \tag{44}$$

Then, the result can be concluded by the same techniques as those used in the proofs of Theorems 1. This completes the proof.  $\square$

In practice, the  $\operatorname{sgn}(\bullet)$  function term “ $\operatorname{sgn}(\bullet)$ ” in Eq. (30) or Eq. (41b) usually leads to an undesirable chattering of when system across the switching surface  $S = 0$ . The chatter is normally undesirable in practice, since it may excite unmodeled high-frequency dynamics, which could result in unforeseen instabilities and may cause damage to actuator mechanisms. This problem can be alleviated by introduction a smooth hyperbolic tangent function, which is defined as

$$\tanh(\beta\sigma) = \frac{e^{\beta\sigma} - e^{-\beta\sigma}}{e^{\beta\sigma} + e^{-\beta\sigma}} \tag{45}$$

Using this approximation, the control law in Eq. (41b) can be modified as

$$\overline{u}_0 = B_2^{-1} (I - \overline{D}_B)^{-1} [-Hw(t) - \Pi|S| - \delta - \eta] \tanh[\beta(S - \chi)] - B_2^{-1} (I + \overline{D}_B)^{-1} \alpha\chi + u_r \tag{46}$$

Note that the hyperbolic tangent function is continuously differentiable (with respect to  $S$ ), and as  $\beta \rightarrow \infty$ , and  $\tanh(\bullet) \rightarrow \operatorname{sgn}(\bullet)$ , so (46a) tends to Eq. (30) or (Eqs. (46b)–(41b)) in the limit. It is being used here to illustrate that a continuous approximation to the discontinuous sliding-mode control law can alleviate undesirable chattering without incurring a significant loss of the performance achieved by the original designed control law.

#### 4. Simulation results

In order to demonstrate the effectiveness of the proposed control schemes, numerical simulations have been performed and presented in this section. The key technical indexes of flexible spacecraft used in the simulation are given in Ref. [28]. Here the first five elastic modes, 3.161, 16.954 s, 47.233, 94.557 rad/s, and 153.003 rad/s with all damping ratios of 0.004, respectively, are considered in the simulation. The first two low-order modes of five are mainly considered in the flexible system for vibration suppression and have been taken into account in the controller design. The reference model used is the normal system with the first two low-order modes of five,  $\omega_{1m} = 3.1613.161$  rad/s and  $\omega_{1m} = 16.95416.954$  rad/s, and the damping ratio  $\zeta_{1m} = \zeta_{2m} = 0.004$ , respectively. In the simulation, it is desired to slew the spacecraft to a target angle  $60^\circ$  and the initial conditions are assumed to be  $(0) = 0, \dot{\theta}(0) = 0, q(0) = 0$  and  $\dot{q}(0) = 0$ . In addition, the flywheel, in practical implementation, restricted by physical structure (saturation), is always behaving as bounded control, with the saturation value 0.5 N m. Note that for the purpose of controller design, first two modes are considered.

The relations between the parametric uncertainty, the actual natural frequencies  $\omega_I$  and the normal natural frequencies  $\omega_{im}$ , can be expressed as follows:

$$|\omega_i^2 - \omega_{im}^2| \delta_A \omega_{im}^2 \quad (i = 1, 2) \tag{47}$$

Assume  $\Delta B = B_m \cdot 0.5 \sin(4t)$ , and the uncertainty input  $D_B = 0.1$  is less than the upper bound of input variation  $\delta_B = 1$ , and the external disturbance  $d(t)$  is a random disturbance torque, given by

$$d(t) = d_{\max} \mathcal{N}(\bullet) \tag{48}$$

whose maximum absolute  $d_{\max}$  has been fixed to 0.1 N m;  $\mathcal{N}(\bullet)$  denotes the normal distribution with mean zero and standard deviation one.

4.1. PID with anti-wind control and its combination with IS

To demonstrate the performance of the vibration control schemes, a proportional plus integral plus derivative (PID) feedback control of collocated sensor signals is first adopted for control of rigid-body motion of the spacecraft. To overcome the saturation problem, anti-wind control (AWC) technique is considered [34]. A block diagram of the PID with AWC is shown in Fig. 3. The corresponding hub angle and velocity of the spacecraft, modal vibrations and the required control torque of response using the PID with AWC are shown in Fig. 4. It is noted that an acceptable hub angle response was achieved. The spacecraft reached the demanded angle with a settling time about 30 s without overshoot. However, a significant amount of vibration occurred during the maneuvering of the flexible spacecraft as demonstrated in Fig. 4(b), in which time response of the first two vibration modes and vibration energy with the maximum amplitude value more than 0.6 N m. Note that the energy function is given by  $E = \dot{q}^T \dot{q} + q^T K_{qq} q$ , and here first five vibration modes are considered. In addition, Here, the time response of control torque without AWC is also shown in Fig. 4(a, dotted line) to show the effectiveness of AWC. Despite the fact that there still exists some room for improvement with different design parameter sets, there is not much improvement in the hub-angle and velocity responses.

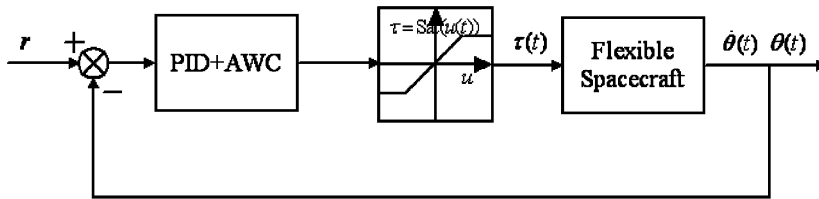


Fig. 3. The PID + AWC structure.

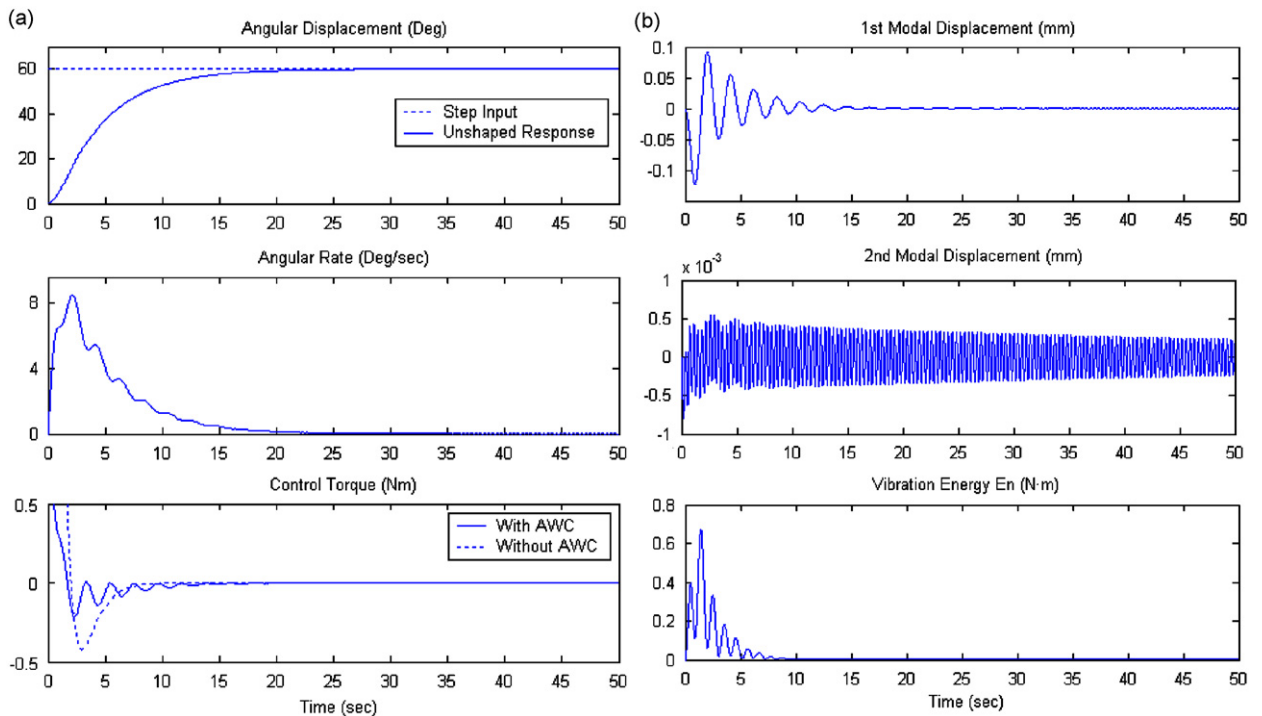


Fig. 4. Time response for using PD + AWC case: (a) time response of angle, rate, and control torque, (b) time responses of vibration displacements and energy.

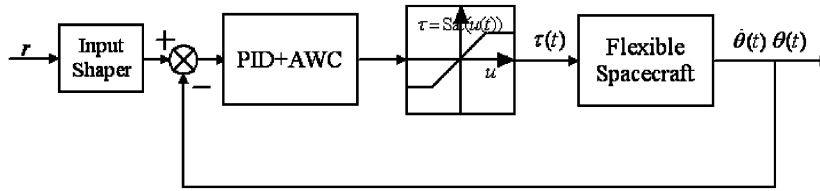


Fig. 5. The PID + AWC with input shaper structure.

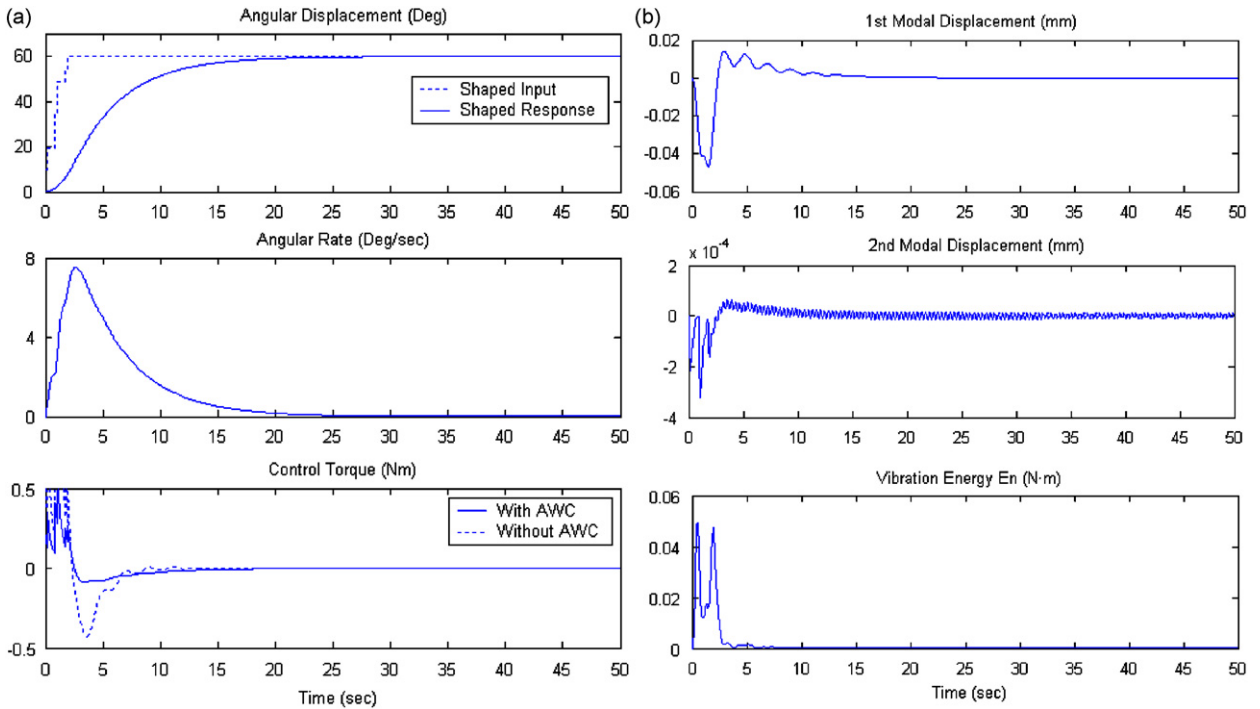


Fig. 6. Time response of using PID+AWC with IS case: (a) time response of angle, rate and control torque, (b) time responses of vibration displacements and energy.

In order to actively suppress the modal vibration, a hybrid control structure for control of rigid-body motion and vibration suppression of the flexible appendages using the saturation compensated PID control with active vibration reduction technique based on shaping is presented here. A block diagram of the hybrid control scheme is shown in Fig. 5. In this case, the PID controller parameters for the attitude control remain the same for a fair comparison, and four impulses ZVDD-shaper for the first-mode and two impulses ZV-shaper for the second-mode are implemented. Fig. 6 shows the results of employing the saturation compensated PID controller with input shaper. It is clear from the top plot of Fig. 6(a) that the imposed desired angular displacement is accurately achieved by employing the hybrid law. The relatively large amplitude vibrations excited by rapid maneuvers can be actively suppressed, as shown in Fig. 6(b), and the energy with less than 0.05 N·m. This reflects the effectiveness of the input shaping for active vibrations suppression.

#### 4.2. VSOFC and its combination with IS

In order to improve the attitude angle response and further reduce the vibrations, the proposed ASMC is adopted here and compared with the saturation compensated PID control case. Fig. 7 shows the results of implementing the proposed variable structure output feedback controller acting on the rigid hub. Note that no

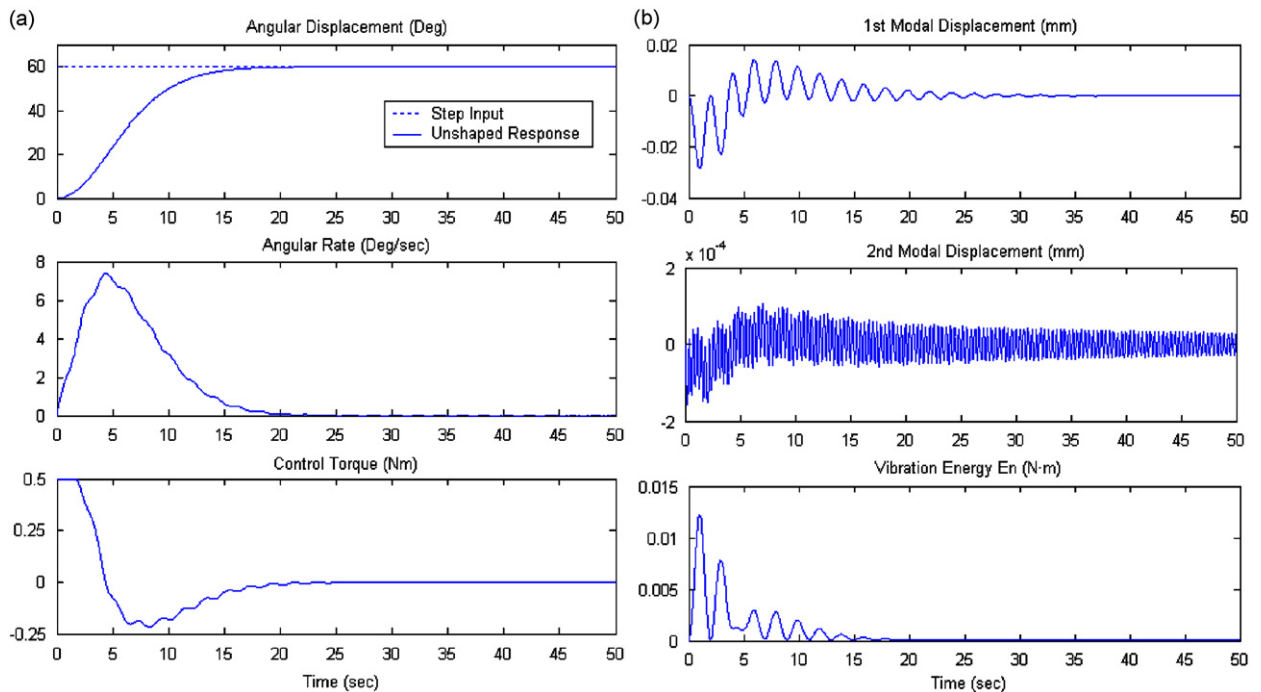


Fig. 7. Time response of using VSOFC without saturation compensator case: (a) time response of angle, rate and control torque, (b) time responses of vibration displacements and energy.

saturation compensation is considered in this case. It is clear from the plot of the top of Fig. 7 that the imposed desired angular displacement is accurately achieved by employing the VSOFC law. From the comparison of Figs. 4 and 7, it is clear that the relatively large amplitude vibrations excited by rapid maneuvers can be passively suppressed, and the inner-torque of each flywheel can approach to zero at the time of 25 s, but there exists control saturation and little chattering.

Even though the proposed controller can passively suppress the relatively large amplitude vibrations induced by rapid maneuvers, some residual micro-vibrations may be present. The case of the proposed controller integrated with input shaper is also studied here. In this case, the VSOFC parameters for the attitude control remain the same for a fair comparison, and four impulses ZVDD-shaper for the first-mode and two impulses ZV-shaper for the second-mode are also implemented. Fig. 8 shows the results of employing this combination. It is clear from the top plot of Fig. 8 that the imposed desired angular displacement is accurately achieved by employing the hybrid law in the presence of the external disturbances. The relatively large amplitude vibrations excited by rapid maneuvers can be actively suppressed, as shown in Fig. 8(b), with less than 0.004 N m in energy. This further demonstrates the validity of active vibration reduction base on the input shaping technique. Moreover, the chattering can also be reduced in some sense.

#### 4.2.1. SOFC with saturation compensator and its combination with IS

For overcoming the saturation problem, the proposed control law in Eq. (41) is also studied in this subsection. The same simulation case is repeated with the control law Eq. (41) replacing the proposed VSOFC for a fair comparison and the results of simulation were shown in Fig. 9. For this case, the imposed desired angular displacement can be achieved, and no saturation phenomenon can be observed in Fig. 9(a). At the same time, in order to eliminate the vibration corresponding to the flexible appendage, the convolved first-mode-ZVDD-shaper and second-mode-ZV-shaper is also used. The plots of this case are shown in Fig. 10. It is clear that, from comparison of Figs. 8 and 10, even if the attitude angle response is improved less, initially a noticeable amount of vibration was observed with the maximum amplitude of the energy being no more than 0.003 N m, and the modal vibration response was found to have almost zero vibration after 30 s. This shows the effectiveness of the saturation compensated VSOFC for the attitude maneuver and the vibration reduction.

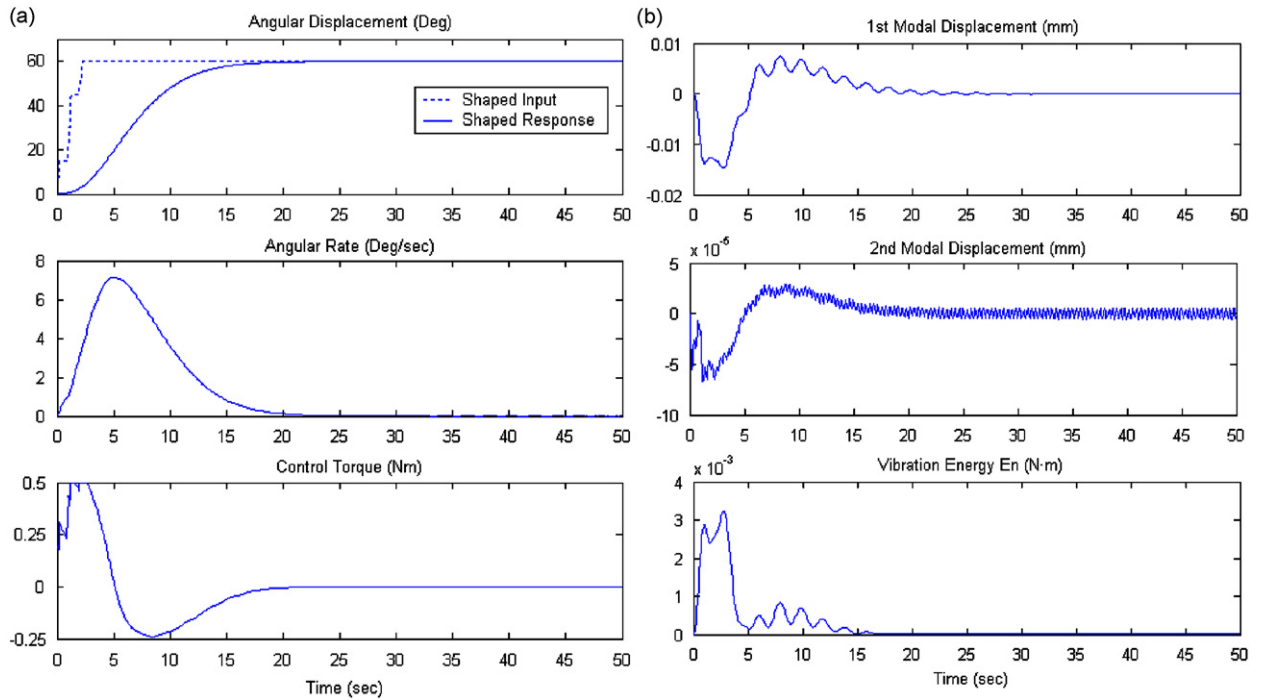


Fig. 8. Time response of using VSOFC without saturation compensator + IS case: (a) time response of angle, rate and control torque, (b) time responses of vibration displacements and energy.

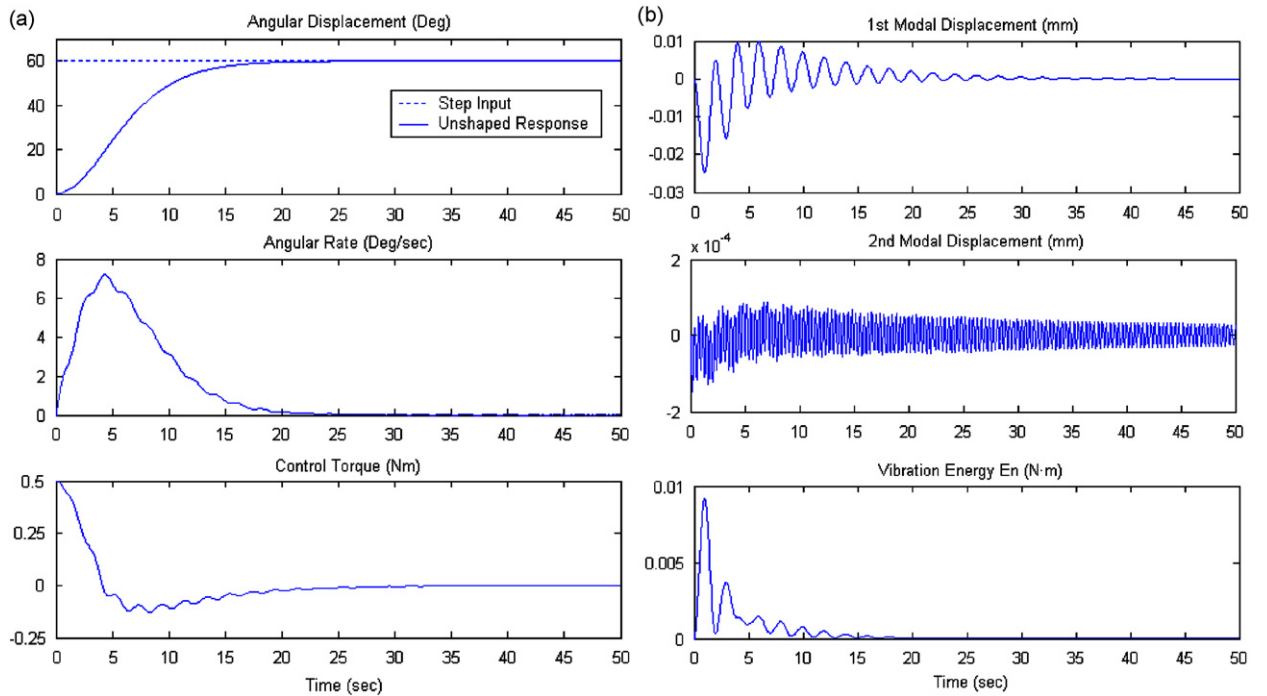


Fig. 9. Time response of using VSOFC with saturation compensator case: (a) time response of angle, rate and control torque, (b) time responses of vibration displacements and energy.

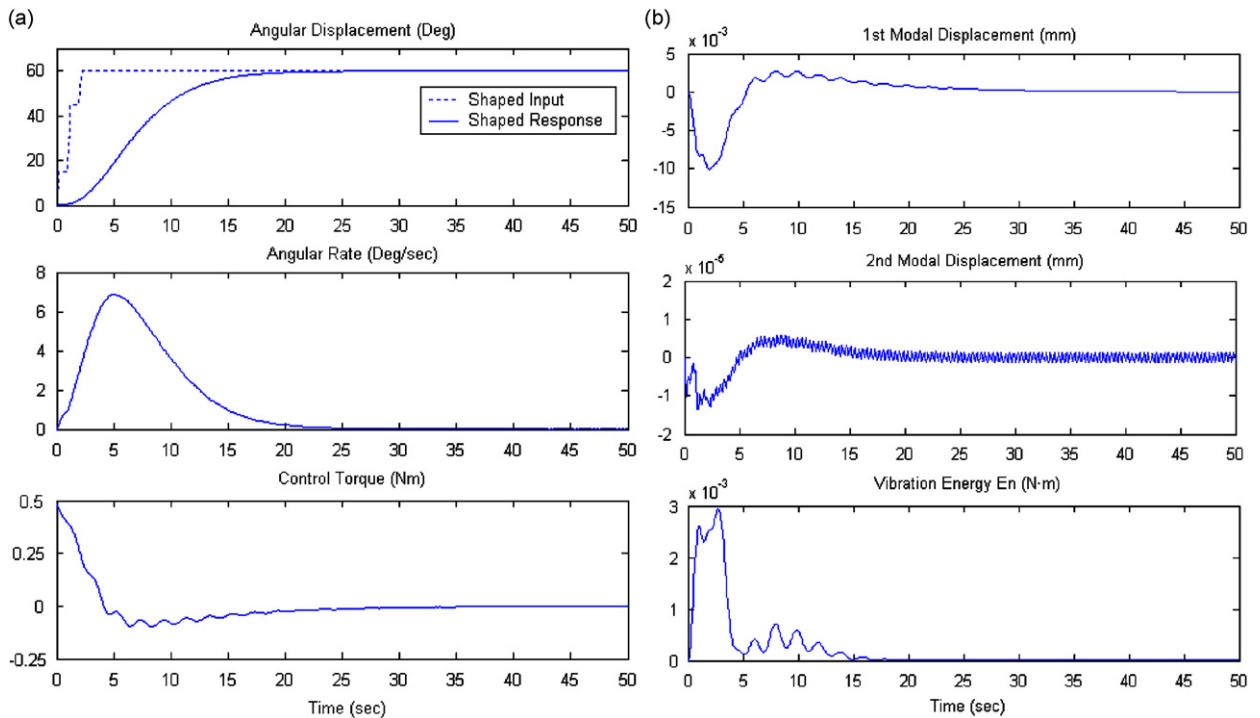


Fig. 10. Time response of using VSOFC with saturation compensator+IS case: (a) time response of angle, rate and control torque, (b) time responses of vibration displacements and energy.

Extensive simulations were also done using different parameters uncertainty, and disturbance inputs. These results show that in the closed-loop system attitude control and vibration stabilization are accomplished in spite of perturbation in the system. Moreover, the flexibility in the choice of control parameters can be utilized to obtain desirable performance while meeting the constraints on the control magnitude and elastic deflection.

From the comparison of above cases, it is shown that the proposed approach cannot only accomplish the attitude control during maneuvers, but also simultaneously suppress the undesired vibrations of the flexible appendages even though the uncertainties and disturbances are explicitly considered. Furthermore, the saturation problem can also be overcome. This control approach provides the theoretical basis for the practical application of the advanced control theory to flexible spacecraft attitude control system.

## 5. Conclusion

In this paper, a new approach for simultaneous vibration reduction and precise pointing control of flexible spacecraft is presented. This approach integrates the method of command input shaping and the theory of VSOFC that takes into account actuator saturation, parameters uncertainties, and even external disturbances provide that the bounded are known. The method of command input shaping is implemented outside of the feedback loop to modify the existing command so that less vibration will be caused by the command itself. The feedback controller based on VSOFC is designed to make the closed-loop system behave like the reference system with input shaper and suppress the vibration of the flexible structures in the presence of parametric uncertainty and external disturbances. For the synthesis of the attitude controller, only the pitch angle and its derivative are used. Moreover, a saturation compensator is also designed to prevent the presence of input saturation from destroying the system performance. To reduce chattering in an implementation, the discontinuous term are replaced by a smoothed control forms and compared by numerical simulation. Simulation results of slew operation of a spacecraft with flexible appendage demonstrate that with the



command input shaper and the variable structure output feedback controller with saturation compensator, the proposed new approach can significantly reduce the vibration of the flexible beam during slew operations.

Our future research directions include the following: (1) extensions of the proposed algorithms to the case of tracking; (2) combination of these algorithms with some active vibration suppression techniques, such as using piezoelectric materials for further reducing the vibration during and after the maneuver operations; and (3) digital implementation of the control scheme on hardware platforms for attitude control experimentation.

## Acknowledgments

This present work was supported by Development Program for Outstanding Young Teachers in Harbin Institute of Technology (HITQNJS.2007.001), Research Fund for the Doctoral Program of Higher Education of China (Project no.: 20070213061) and National Natural Science Foundation of China (Project no.: 60774062). The author fully appreciates the financial support. The author would also like to thank the reviewers and the Editor for many suggestions that helped to improve the paper.

## References

- [1] G. Singh, P.T. Kabamba, N.H. McClamroch, Bang–bang control of flexible spacecraft slewing maneuvers: guaranteed terminal pointing accuracy, *Journal of Guidance, Control and Dynamics* 13 (1990) 376–379.
- [2] T. Nagata, V.J. Modi, H. Matsuo, Dynamics and control of flexible multibody systems—part II: simulation code and parametric studies with nonlinear control, *Acta Astronautica* 49 (2001) 595–610.
- [3] F. Karray, A. Grewal, M. Glaum, V. Modi, Stiffening control of a class of nonlinear affine system, *IEEE Transactions on Aerospace and Electronic Systems* 33 (2) (1997) 473–484.
- [4] A. Grewal, V.J. Modi, Robust attitude and vibration control of the space station, *Acta Astronautica* 38 (3) (1996) 139–160.
- [5] S.R. Vadali, Variable structure control of spacecraft large attitude maneuvers, *Journal of Guidance, Control and Dynamics* 9 (3) (1986) 235–239.
- [6] T.A.W. Dwyer, H. Sira-Ramirez, Variable structure control of spacecraft attitude maneuver, *Journal of Guidance, Control and Dynamics* 11 (3) (1988) 262–270.
- [7] J.L. Crassidis, F.L. Markley, Sliding mode control using modified Rodrigues parameters, *Journal of Guidance, Control and Dynamics* 19 (6) (1996) 1381–1383.
- [8] S.C. Lo, Y.P. Chen, Smooth sliding mode control for spacecraft attitude tracking maneuvers, *Journal of Guidance, Control and Dynamics* 18 (6) (1995) 1345–1349.
- [9] A. Iyer, S.N. Singh, Variable structure slewing control and vibration damping of flexible spacecraft, *Acta Astronautica* 25 (1) (1991) 1–9.
- [10] S.N. Singh, Robust nonlinear attitude control of flexible spacecraft, *IEEE Transactions on Aerospace and Electronic Systems* 23 (3) (1987) 380–387.
- [11] H.o. Oz, O. Mostafa, Variable structure control systems maneuvering of flexible spacecraft, *Journal of the Astronautical Sciences* 36 (3) (1988) 311–344.
- [12] Q.L. Hu, G.F. Ma, Control of three-axis stabilized flexible spacecrafts using variable structure strategies subject to input nonlinearities, *SAGE Journal of Vibration and Control* 12 (6) (2006) 659–681.
- [13] Y. Zeng, A.D. Araujo, S.N. Singh, Output feedback variable structure adaptive control of a flexible spacecraft, *Acta Astronautica* 44 (1) (1999) 11–22.
- [14] S.N. Singh, R. Zhang, Adaptive output feedback control of flexible with flexible appendages by modeling error compensation, *Acta Astronautica* 54 (2004) 229–243.
- [15] A.S. Lewis, Robust output feedback using sliding mode control, *Journal of Guidance, Control and Dynamics* 24 (5) (2001) 873–878.
- [16] J.D. Bošković, S.M. Li, R.K. Mehra, Robust tracking control design for spacecraft under control input saturation, *Journal of Guidance, Control and Dynamics* 27 (4) (2004) 627–633.
- [17] P. Tsiotras, J. Luo, Control of under-actuated spacecraft with bounded inputs, *Automatica* 36 (8) (2000) 1153–1169.
- [18] R.D. Robinett, G.D. Parker, H. Schaub, J.L. Junkins, Lyapunov optimal saturated control for nonlinear systems, *Journal of Guidance, Control and Dynamics* 20 (6) (1997) 1083–1088.
- [19] R.J. Wallsgrove, M.R. Akella, Globally stabilizing saturated attitude control in the presence of bounded unknown disturbances, *Journal of Guidance, Control and Dynamics* 28 (5) (2005) 957–963.
- [20] H.C. Bang, M.J. Tahk, H.D. Choi, Large angle attitude control of spacecraft with actuator saturation, *Control Engineering Practice* 11 (2003) 989–997.
- [21] N. Singer, W. Seering, Preshaping command inputs to reduce system vibration, *Journal of Dynamic Systems, Measurement and Control—Transactions of the ASME* 112 (1990) 76–82.
- [22] W. Singhose, A. Banerjee, W. Seering, Slewing flexible spacecraft with deflection-limiting input shaping, *Journal of Guidance, Control, and Dynamics* 20 (2) (1997) 291–298.

- [23] A. Banerjee, W. Singhose, Command shaping for nonlinear tracking control of a two-link flexible manipulator, *Journal of Guidance, Control, and Dynamics* 21 (6) (1998) 1012–1015.
- [24] K. Hillsley, L.S. Yurkovich, Vibration control of a two-link flexible robot arm, *Journal of Dynamics and Control Systems* 16 (2) (1993) 261–280.
- [25] K. Hillsley, L.S. Yurkovich, Vibration control of a two-link flexible robot arm, *IEEE International Conference on Robotics and Automation* 4 (1991) 2121–2126.
- [26] P.H. Chuang, H.S. Park, Time-varying input shaping technique applied to vibration reduction of an industrial robot, *Control Engineering Practice* 13 (2005) 121–130.
- [27] J.J. Shan, H.T. Liu, D. Sun, Modified input shaping for a rotation single-link flexible manipulator, *Journal of Sound and Vibration* 285 (2005) 187–207.
- [28] Q.L. Hu, G.F. Ma, Vibration suppression of flexible spacecraft during attitude maneuvers, *Journal of Guidance, Control, and Dynamics* 28 (2) (2005) 377–380.
- [29] D. Gorinevsky, G. Vukovich, Nonlinear input shaping control of flexible spacecraft reorientation maneuver, *Journal of Guidance, Control, and Dynamics* 21 (2) (1998) 227–264.
- [30] F.C. Craig, Y.P. Lucy, Adaptive input shaping for maneuvering flexible structures, *Automatica* 40 (2004) 685–693.
- [31] W.J. Wang, Y.T. Fan, New output feedback design in variable structure systems, *Journal of Guidance, Control and Dynamics* 17 (2) (1994) 337–340.
- [32] C.M. Kwan, Sliding control using output feedback, *Journal of Guidance, Control and Dynamics* 19 (3) (1996) 731–733.
- [33] J. Slotine, W. Li, *Applied Nonlinear Control*, Prentice-Hall, Upper Saddle River, NJ, 1991.
- [34] M.V. Kothare, P.J. Campo, M. Morari, C.N. Nett, A unified framework for the study of anti-windup designs, *Automatica* 30 (1994) 1869–1883.